Time-Temperature-Transformation Measurements of FePt Thin Films in the Millisecond Regime Using Pulse Laser Processing

Gregory B. Thompson – The University of Alabama
et. al

Citation of published version:

Inaba, Y., et al. (2010): Time-Temperature-Transformation Measurements of FePt Thin Films in the Millisecond Regime Using Pulse Laser Processing. *Journal of Applied Physics*, 108(10). DOI: https://doi.org/10.1063/1.3506689

Time-temperature-transformation measurements of FePt thin films in the millisecond regime using pulse laser processing

Yuki Inaba,[1] Iulica Zana,[1,2] Caleb Swartz,[3] Yukiko Kubota,[4] Tim Klemmer,[4] J. W. Harrell,[1,5,a)] and Gregory B. Thompson[1,6]
[1]*Center for Materials and Information Technology, The University of Alabama, Tuscaloosa, Alabama 35487, USA*
[2]*Western Digital, Fremont, California 94538, USA*
[3]*Belmont University, Nashville Tennessee 37212, USA*
[4]*Seagate Technologies, Fremont, California 94538, USA*
[5]*Department of Physics and Astronomy, The University of Alabama, Tuscaloosa, Alabama 35487, USA*
[6]*Department of Metallurgical and Materials Engineering, The University of Alabama, Box 870202, Tuscaloosa, Alabama 35487, USA*

(Received 11 July 2010; accepted 28 September 2010; published online 19 November 2010)

A section of the time-temperature-transformation (TTT) curve has been measured in the millisecond regime to describe the A1 to $L1_0$ transformation of 10 nm FePt thin films. Short time annealing was accomplished using a pulsed neodymium-doped yttrium aluminum garnet laser operating at a wavelength of 1064 nm. The temperature-time profile of the films was measured using an optical pyrometer and a platinum thin film resistor and it was numerically modeled. Effective thermal pulse widths were determined from the time dependence of the atomic diffusion coefficient calculated from the measured temperature profile. The measured TTT diagram involving average order parameter is consistent with theoretical predictions of TTT diagrams involving ordered volume fraction and shows that partial ordering can be obtained with a single effective thermal pulse as short as 1.1 ms. © *2010 American Institute of Physics*. [doi:10.1063/1.3506689]

I. INTRODUCTION

FePt with the magnetically hard $L1_0$ phase is a candidate material for ultrahigh density perpendicular magnetic recording media applications because of its high magnetocrystalline anisotropy.[1] Currently, heat treatments above 500 °C in the time regime of minutes to tens of minutes are conducted to phase transform from A1 to the magnetically hard $L1_0$ ordered phase. Usually, this annealing is accompanied by undesired grain growth, destroying the narrow grain size distribution necessary for ultrahigh-density magnetic media applications.

Recent modeling predicts that the ordering phase transformation can commence on the time scale of 10 to 100s of milliseconds depending on the temperature.[2,3] We have previously reported the effect of laser annealing on the $L1_0$ ordering and grain growth of continuous FePt films deposited on Si or glass substrates at these time scales.[4,5] Magnetic and structural changes were measured as functions of delivered energy fluence.

In this paper, the time-temperature profile resulting from a laser pulse has been both modeled and measured providing better comparison to previous modeling predictions.[3] The results show that the choice of substrate can have a significant effect on the time-temperature profile and that a glass substrate allows for a much faster cooling rate than silicon. Consequently, the pulse laser annealing experiments presented here have focused on FePt films deposited onto glass. In addition, the effective annealing times resulting from the laser pulses have been calculated from the time dependence of the atomic diffusion coefficient. The coercivity and order parameter have been measured as a function of peak temperature and time, and an experimentally constructed section of the time-temperature-transformation (TTT) diagram has been plotted in the millisecond regime and compared with predictions.[3]

II. EXPERIMENTAL DETAILS

For laser processing, 10 nm FePt films were deposited onto Corning 1737 2 in. square glass substrates[6] by dc sputtering with commercially pure (99.5%) elemental Fe and Pt targets in an AJA ATC-1500 magnetron sputtering system. The base pressure was $<5\times10^{-8}$ Torr prior to sputtering at which point ultrahigh-purity Ar was admitted at a flow rate of 10 standard cubic centimeters per minute into the chamber to a pressure of 2 mTorr. The films consisted of the structure Si_3N_4(5 nm)/FePt(10 nm)/Si_3N_4(5 nm)/glass substrate. The FePt film was deposited as a $[Fe(\sim0.24\ nm)/Pt(\sim0.3\ nm)]_{22}$ multilayer; however, atom probe tomography studies of similar multilayered films deposited with the same system under the same conditions have shown that the layers are highly intermixed in the as-deposited state and have a nearly equiatomic composition of FePt.[7] The equiatomic composition was confirmed by scanning transmission electron microscopy (TEM)-x-ray energy dispersive spectroscopy analysis. A Si_3N_4 composite target was used to grow the Si_3N_4 layers by RF sputtering. The Si_3N_4 acts as a diffusion barrier to prevent any undesired substrate or atmospheric reactions with the FePt thin film during annealing.

a)Electronic mail: jharrell@bama.ua.edu.

Post deposition, the substrate with film was cut into 5 mm $\times$5 mm squares for laser and furnace annealing and characterization.

For temperature measurements, a thin film resistance thermometer was made by depositing a similar film structure with 10 nm of Pt in place of the FePt film. The real and imaginary parts of the index of refraction, n and k, of Pt and FePt at 1064 nm are very similar. For Pt, $n=3.67$ and $k=5.94$,[8] and for FePt, $n\sim3.6$ and $k\sim5.0$.[9] The laser absorbance, A, calculated using these values are nearly the same.[10] For Pt, $A(\text{calc})=0.37$, and for FePt, $A(\text{calc})=0.39$. The absorbance was also experimentally determined by measuring the transmittance, T, and reflectance, R, $(A=1-R-T)$ using a 15 mW cw laser at a wavelength of 980 nm. For Pt, $A(\text{meas})=0.38\pm0.2$, and for FePt, $A(\text{meas})=0.39\pm0.2$. The heat capacity and thermal conductivity are also very similar;[11–13] however, for millisecond pulses the peak temperature is essentially independent of these latter film properties. (As will be discussed later, it depends strongly on the thermal properties of the substrate.) Thus, the temperature response to the laser pulses is expected to be nearly the same in Pt and FePt thin films. The resistance of the FePt film could not be used as a temperature monitor since the film undergoes a phase transformation and grain growth during the annealing. These structural changes would complicate the temperature dependence of the resistance of the film. The Pt film was preannealed so that the film resistance showed reliable and reproducible behavior. All layers were deposited with a four-point mask to form contacts for the resistance measurements. To measure resistance, the current was supplied by a KEITHLEY 6200 current source and the voltage was measured using either a KEITHLEY 2700 multimeter (for steady-state measurements) or a digital oscilloscope (for transient measurements). A Laytek, Marathon-MM-2 ML optical pyrometer with a response time of 2 ms was also used to qualitatively measure the time-temperature profile. The absolute temperature could not be measured with the pyrometer since the effective emissivity of the thin film was not known.

An Electrox Scorpion neodymium-doped yttrium aluminum garnet (Nd:YAG) laser with a wavelength of 1064 nm was used to anneal the FePt thin films. The samples were placed on a Corning MACOR machineable glass ceramic holder with a circular hole underneath the sample. The hole minimized the contact with the sample holder to less than 0.5 mm at the corners of the substrate. Thermal annealing was done in air using a single pulse with a pulse width of 2.5, 5.0, 7.5, or 10 ms. The pulse width was controlled by a mechanical shutter in the laser, and the laser energy fluence was varied from 0 to 10 J/cm^2. To minimize potential delamination or thermal shock because of thermal expansion differences between the film and the substrate during the laser pulse, the FePt films were preheated at a temperature of 200 °C using a quartz lamp positioned under the ceramic mount. For the Pt films, the preheat temperature was 150 °C.

The Si_3N_4 layer was effective in preventing damage to the FePt film from the laser pulse. A TEM cross-section foil was prepared using a standard *in situ* extraction focus ion beam (FIB) milling procedure[14] using a FEI Quanta 3D dual electron and FIB microscope. The foil was analyzed in a FEI F20 TEM. The cross section, Fig. 1, of a film that was annealed with a 10 J/cm^2 laser pulse for 10 ms (peak temperature ~700 °C) shows that the silicon nitride barrier layer remained intact and continuous over the surface. Additionally, the FePt film does not indicate agglomeration over the viewed area. Previous laser anneals of similar films has shown that the film does not agglomerate but remain continuous at high pulse energies and produces a mazelike microstructure.[15]

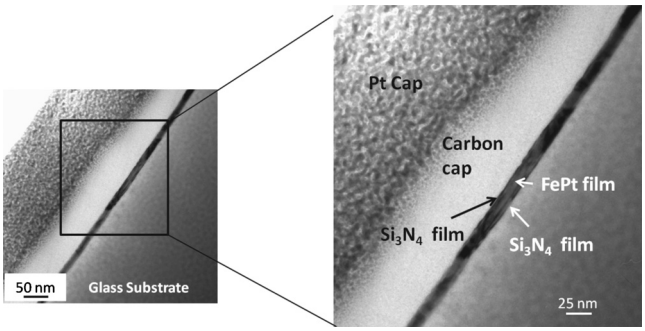

FIG. 1. A bright field TEM cross section of a film annealed with a 10 J/cm^2, 10 ms laser pulse. The capping layers of the silicon nitride and magnetic films are shown. The film appears continuous and does not appear to agglomerated postannealing. The carbon and platinum caps provided a protective surface during the FIB milling. The dark regions in the film are a result of diffraction contrast of the columnar grain structure. Careful observation reveals a film diffraction contrast line parallel to the substrate showing the distinct film layers between the silicon nitride and magnetic film interfaces. Since the substrate was amorphous glass, tilting to a zone axis to ensure the beam is normal to the cross-section could not be accomplished; thus any small thickness discrepancy in the projected image via the scale marker for the micrograph and those reported in the paper is explained.

X-ray diffraction (XRD) spectra were collected using a Bruker D8 discovery general area diffraction detection system using Co $K\alpha$ radiation ($\lambda=1.790$ Å) at 40 keV and 35 mA, and a Philips XRD using Cu $K\alpha$ radiation ($\lambda=1.541$ Å) at 45 kV and 40 mA. In-plane hysteresis loops were measured with a Princeton Instruments Model 2900 alternating gradient magnetometer with a maximum applied field of 18 kOe.

III. THERMAL TRANSPORT MODELING

The intensity profile of the laser pulse on the film was measured and found to vary by less than 20% over the area of the film (5 mm$\times$5 mm). Consequently, the thermal transport was assumed to be approximately one-dimensional. The temperature of the sample during and after the laser pulse as a function of time and normal distance from the surface is given as a solution to the equation[16]

$$\rho C_p \frac{\partial T(x,t)}{\partial t} - K\frac{\partial^2 T(x,t)}{\partial x^2} = Q, \tag{1}$$

where ρ is the mass density, C_p the specific heat, K the thermal conductivity, and Q the heat source (W/m^3). For the film on a glass substrate, the heat source is the laser energy absorbed in the metal film. Absorption in the substrate and Si_3N_4 layers[17] is negligible. For the Si substrate, absorption

TABLE I. Optical and thermal properties of the substrates at a wavelength of 1064 nm used in the calculations.

	Glass	Si
Density, ρ (kg/m^3)	2540[a]	2330[b]
Heat capacity, C (J/kg K)	1100[a]	143 $T^{0.275}$ [c]
Thermal conductivity, K (W/m K)	1.4[a]	(4.4×10^5) $T^{-1.376}$ [d]
Refractive index, n	1.51[a]	3.56[e]
Extinction coefficient, k	0[a]	0[e]
Absorption coefficient, α (1/m)	0[a]	935[e]

[a]Reference 6.
[b]Reference 30.
[c]Reference 31.
[d]Reference 32.
[e]Reference 33.

in Si must also be considered. (See Table I for substrate parameters.)

The heat source is given by

$$Q = I \times f(t) \times \alpha \times \exp(-\alpha x), \tag{2}$$

where I is the net flux (W/m^2) entering the film, $f(t)$ is the temporal shape of the laser pulse (assumed to be square), α is the absorption coefficient (m^{-1}), and x is the normal distance into the absorbing layer (m). The net flux entering the film is given by

$$I = I_0(1-R), \tag{3}$$

where I_0 is the incident flux and R is the reflectance. The reflectance, R, transmittance, T, and absorbance, $A(=1-R\text{-}T)$, for the film can be calculated from the real and imaginary parts of the index of refraction of the absorbing film and the substrate and from the thickness of the film using the method described by Heavens.[10] Fig. 2 shows T, R, and A as a function of film thickness for Pt on glass. At the film thickness of 10 nm, $T=0.20$, $R=0.43$, and $A=0.37$. Curves qualitatively similar to those in Fig. 2 were obtained for Pt on Si. The dependence of the absorptance on film thickness in Fig. 2 is quite similar to that measured by Mahan and Marple[18] for Pt on Si at a wavelength of 3390 nm, which also shows enhanced absorptance at a thickness of less than 10 nm.

The effective absorption coefficient, α, can be calculated from A using the relationship

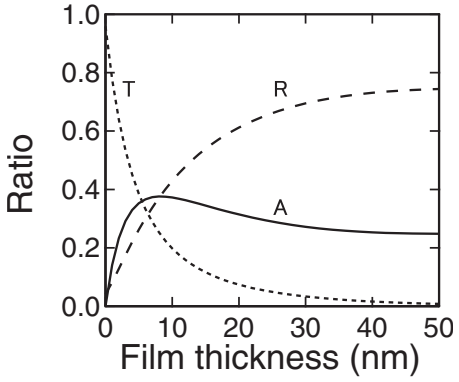

FIG. 2. Transmittance (T), reflectance (R), and absorptance (A) of Pt on glass substrate as a function of Pt film thickness.

$$A = (1-R)(1-e^{-\alpha h}), \tag{4}$$

where h is the film thickness. This yields $\alpha=1.05\times10^8$/m, which is larger than the bulk value given by $\alpha(\text{bulk}) = 4\pi k/\lambda = 7.0\times10^7$/m. The calculated effect of the thin, nonabsorbing Si_3N_4 layers on the reflectance is negligible.[10]

The boundary conditions at the film and substrate interfaces are such that the temperature and the heat flow are continuous.

The outer surface of the film and substrate cool by a combination of convection, radiation, and contact of the substrate with the sample holder. The relative importance of convection and conduction depends on the value of the convection coefficient for air, which depends on experimental conditions but is nominally less than about 50 W/m^2 K.[19,20] For a convection coefficient of 50 W/m^2 K, the initial convective and radiative cool-down rates of the substrate at a peak temperature of 700 °C are comparable, and the time for the celsius temperature to drop by a factor of two is about 6 s. As will be discussed later, conduction to the sample holder is likely the dominant cool-down process for the substrate.

Because of its high thermal diffusivity and small thickness, the temperature of the Pt film is essentially spatially uniform during the laser pulse. For a single absorbing layer on a nonabsorbing substrate, it can be shown for a square laser pulse profile that the film temperature during the pulse is given by[11,16,21]

$$T = T_0 + \frac{2}{\sqrt{\pi}}\frac{I_0 A}{\sqrt{\rho C_s K_s}}\sqrt{t}, \tag{5}$$

where T_0 is the initial film and substrate temperature, ρ is the mass density of the substrate, C_s is the specific heat of the substrate, K_s is the thermal conductivity of the substrate, and t is the laser pulse width. The temperature of the film during cool down is given by[21]

$$T = T_0 + \frac{2}{\sqrt{\pi}}\frac{I_0 A}{\sqrt{\rho C_s K_s}}(\sqrt{t} - \sqrt{t-t_p}), \tag{6}$$

where t_p is the laser pulse width. Equations (5) and (6) assume a semi-infinite substrate and neglect external heat loss from the surfaces. These are found to be good approximations during the pulse and for several pulse widths following the pulse. Equation (5) shows that the peak temperature for a single absorbing layer on glass depends only on the net energy absorbed in the film and the thermal properties of the substrate, which determine the rate at which this energy is transported from the film into the substrate.

The temperature of the Pt film on Si during the laser pulse can be estimated by assuming that all the laser energy absorbed by the Pt and by the Si quickly diffuses to yield a uniform temperature and that the heat loss during the pulse is negligible. In this case,

$$T = T_0 + \frac{I_0 A t}{\rho_s d_s C_s}, \tag{7}$$

where d_s is the thickness of the substrate and A includes both film and substrate absorption. Unlike the film on glass, the cool-down time of the film on Si will be long compared to

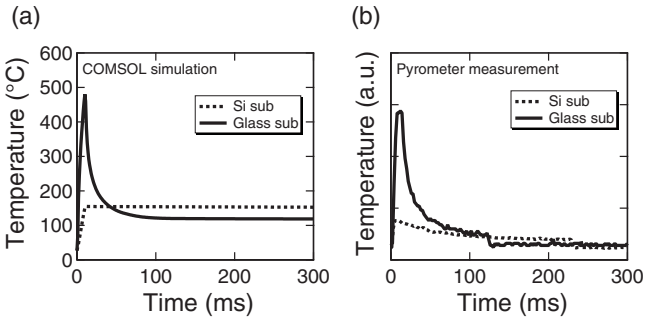

FIG. 3. Time-temperature profile obtained with (a) COMSOL simulation and (b) pyrometer measurement with the same power setting of 2×10^7 W/m^2.

the laser pulse width and will be controlled by surface losses (convection, radiation, and conduction to sample support) from the film and substrate.

The transient temperature was also calculated using the finite element program COMSOL (Ref. 22) assuming surface cooling by convection. Figure 3(a) shows the calculated time-temperature profile of the Pt film on glass and on Si resulting from a 10 ms laser pulse with an intensity of 2×10^7 W/m^2. The temperature-time profiles determined from the COMSOL calculations are in good agreement with Eqs. (5)–(7).

The peak temperature of the film is much higher and the cool-down time of the film is much shorter on glass than on Si. The difference in the substrate effect is because of the much larger thermal conductivity of Si (Table I) and, to a lesser extent, the fact that Si absorbs some of radiation while glass is nonabsorbing. The high diffusivity of the Si allows the heat absorbed in the Pt film to quickly diffuse into the substrate during the laser pulse. The film and Si substrate are nearly in thermal equilibrium during and after the pulse. This has the effect of reducing the peak temperature and increasing the cool down time of the film since both the film and substrate must cool nearly simultaneously. On the other hand, because of the lower thermal diffusivity of the glass and the fact that it is nonabsorbing, the glass heats up much less than the Si during the pulse and acts as a heat sink for the film after the pulse, allowing a more rapid cool-down of the film.

Figure 3(b) shows time-temperature profiles measured with the optical pyrometer for the same conditions as in Fig. 3(a). As previously mentioned, the absolute temperature could not be determined since calibration of the pyrometer requires knowing the emissivity of the film which is less than the bulk value. Qualitatively, the measured and calculated profiles are in good agreement. (The step in the curves at low temperature—at a time of about 125 ms for glass—occurs because the IR emission from the film drops below the response threshold of the pyrometer.) The measured cool-down time of the film on Si is shorter than calculated based on convective and radiative cooling, although still much longer than on glass. A possible explanation for the discrepancy in calculated and measured cool down times with Si is that the Si substrate, because of its large thermal diffusivity, may cool by lateral conduction to the corners of the substrate which rest on the sample holder during the laser processing.

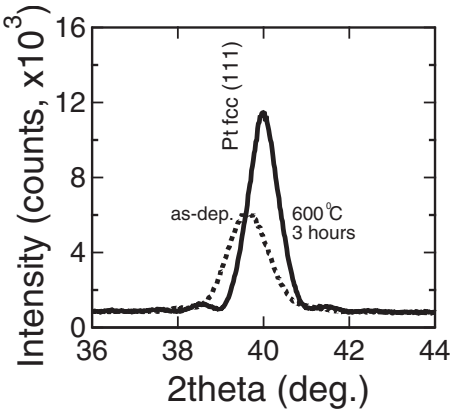

FIG. 4. XRD profile for as-deposited and 600 °C, 3 h heat-treated Pt thin film resistance.

The characteristic time for this lateral thermal diffusion is $t=x^2/(2D_t)$, where x is the sample radius and $D_t=K/(\rho C)$ is the thermal diffusivity for Si. Using, $x=2$ mm and $D_t=2\times10^{-5}$ m^2/s (Table I) gives a diffusion time of 0.1 s, which is comparable to the measured cool down time in Fig. 3(b). Both the calculated and measured temperature profiles demonstrate that the glass substrate is more appropriate for minimizing the duration of the thermal pulse in the millisecond regime.

IV. RESULTS AND DISCUSSION

A. Pt thin film temperature measurements

As described earlier, the Pt thin film was used as a resistance thermometer to determine the film temperature as a function of time during and after the laser pulse. The film was pre-annealed in a furnace at 600 °C for 3 h in order to improve the linearity and reproducibility of the temperature dependence of resistance. Figure 4 shows the θ-2θ XRD spectrum of the Pt film before and after annealing. After annealing, the (111) peak narrows and shifts to a higher angle, suggesting grain growth and a reduction in film stress.

Figure 5 shows the resistance of the Pt film as a function of temperature before and after annealing. The temperature was measured in a steady-state condition with a thermocouple attached near the film. Before preannealing, the resistance increased nonlinearly with temperature, presumably

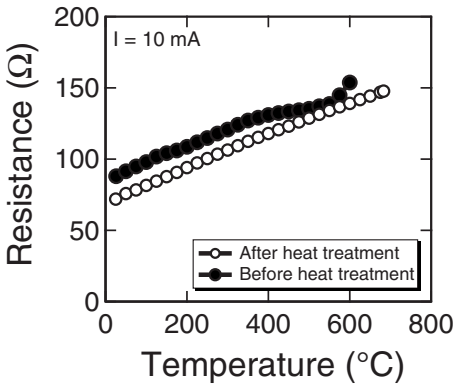

FIG. 5. Temperature dependence of resistance of Pt film before and after heat treatment.

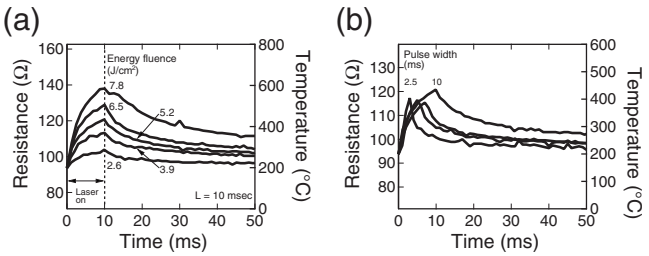

FIG. 6. Time-resistance profile for Pt film obtained with (a) different energy fluences with a fixed pulse width of 10 ms and (b) different pulse widths with fluence adjusted to give nearly the same peak resistance. The right vertical axis represents the converted temperature using the data in Fig. 3.

because of grain growth and release of film stress. After annealing at 600 °C for 3 h, the resistance was lower and the response was much more linear.

Figure 6 shows the resistance-time profiles for the Pt film for different laser pulse widths and fluences. The figure also shows the corresponding temperatures calculated from the calibration curve in Fig. 5. (The film was preheated to 150 °C and the curves were offset by an additional 50 °C to correspond with the 200 °C preheat of the FePt films.) Fig. 6(a) shows profiles for a fixed pulse width of 10 ms for different values of laser fluence, while Fig. 6(b) shows profiles for different pulse widths with the fluences adjusted to give approximately the same peak temperature. These profiles are very similar to the calculated curves and those measured with the optical pyrometer.

Measured and calculated peak temperatures are shown as a function of laser fluence in Fig. 7. The measured peak temperatures correspond to laser pulse widths of 2.5, 5.0, 7.5, and 10 ms. For a given value of fluence, the peak temperature increases as the pulse width decreases. This is expected since the shorter pulses allow less time for the energy absorbed by the film to diffuse into the substrate. Specifically, for a fixed fluence F, $I_0=F/t$, so $T_p \sim 1/\sqrt{t}$.

The calculated temperatures were obtained using Eq. (5) for a fixed pulse width of 10 ms. The calculated temperature increases are smaller than the measured values for the 10 ms pulses by a factor of approximately two. The reason for this discrepancy is not fully understood. The peak temperature is directly proportional to the incident laser intensity I_0 and the

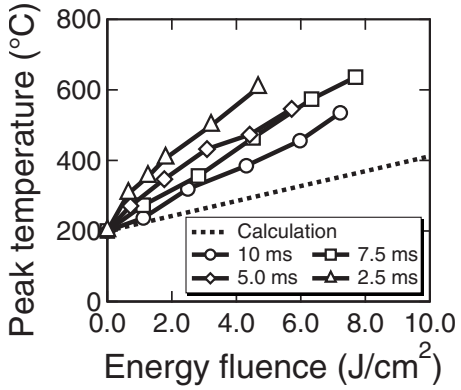

FIG. 7. Peak temperature dependence on energy fluence obtained with various pulse widths. Calculated results obtained with 10 ms pulse width are shown for comparison.

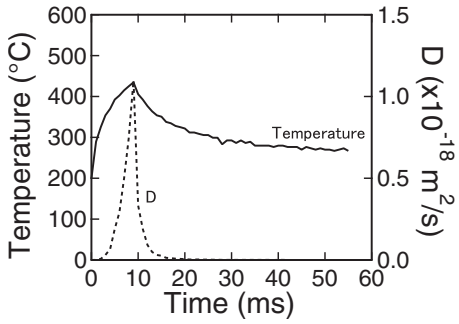

FIG. 8. Temperature and atomic diffusion pulse widths generated by a 10 ms square laser pulse.

absorptance A, so uncertainties in these quantities could be a factor. Thermal interfacial resistance between the film and the substrate can also lead to higher film temperatures.[23] Interfacial resistance can be caused by imperfect contact in the as-deposited films or partial film separation induced by the intense laser pulse. The measured temperatures, however, are expected to be reasonably accurate and these temperatures are used in the following discussions.

B. Effective thermal pulse width

Although the laser pulse itself has a well-defined width, with rise and fall times less than 1 ms, the width of the temperature pulse in the film is not as well defined. While the time for the film temperature to fall to its original value is quite long, the effective thermal pulse can be shown to be quite short since most of the atomic diffusion occurs near the peak temperature. The diffusion coefficient can be written as

$$D = D_0 \exp\left(-\frac{E_a}{k_B T}\right), \tag{8}$$

where D_0 is the pre-exponential factor, E_a the activation energy, k_B the Boltzmann constant, and T the absolute temperature. Using the reported values for interlayer diffusion in Fe/Pt multilayers of $D_0=1.37\times10^{-6}$ m^2/s and $E_a=1.7$ eV,[24] the time dependent diffusion resulting from the laser pulse was calculated. Figure 8 shows the measured temperature profile and the corresponding diffusion coefficient profile for a 10 ms laser pulse.

The mean-square diffusion distance during and after the laser pulse can be calculated as

$$\overline{x^2} = 2\int D(t)dt. \tag{9}$$

The effective pulse width can be defined as the width of a square pulse at the peak temperature, T_p, which gives this same mean-square diffusion distance. That is,

$$\overline{x^2} = 2D(t_p)t_{eff}, \tag{10}$$

where $D(t_p)$ is the maximum diffusion coefficient. For the 10 ms laser pulse (Fig. 8), $t_{eff}=3.4$ ms. The effective pulse width varies slightly with peak temperature and with the value of the diffusion coefficient. Average effective pulse widths for the 2.5, 5.0, 7.5, and 10 ms laser pulses are 1.1 ms, 2.0 ms, 2.7 ms, and 3.8 ms, respectively. The actual

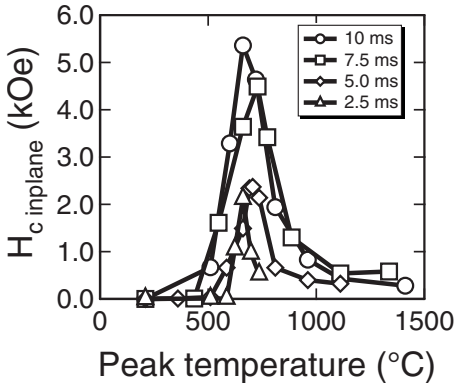

FIG. 9. In-plane coercivity dependence on temperature for different pulse widths.

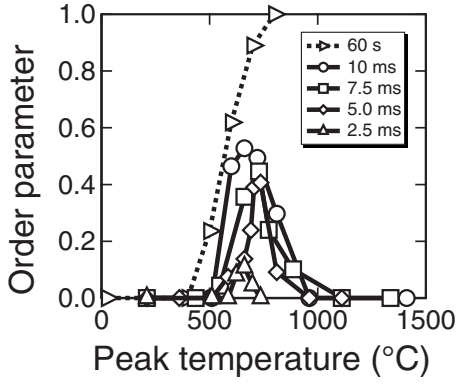

FIG. 10. Order parameter dependence on temperature for different pulse widths and for furnace anneal.

effective pulse widths may be somewhat smaller since the time resolution of the measurements is 1 ms. For a perfectly square laser pulse, the calculated effective diffusion times would be smaller than those calculated for the actual laser pulse by a factor of about two. For the shortest pulse (t_{eff} = 1.1 ms), the root-mean-square diffusion distance is about 2.2 nm at a peak temperature of 700 °C, which is the approximate temperature where maximum ordering occurs. This diffusion distance seems sufficiently large compared with the lattice constant of FePt (~0.38 nm) to allow for short-range diffusion necessary in this polymorphic phase transformation.

The effective thermal pulse width depends on the choice of activation energy for diffusion and does not depend on the pre-exponential factor. Various activation energies have been reported for diffusion in FePt, depending on the diffusing element (Fe, Pt, or interdiffusion at Fe/Pt interfaces), the phase (A1 or $L1_0$), the crystallographic orientation, and the microstructure. For example, the activation energy for self-diffusion of Fe in $L1_0$ films has been reported as 1.65 eV,[25] which would yield an effective diffusion pulse width of 3.5 ms for a 10 ms laser pulse. An activation energy of 3.0 eV has been reported for the self-diffusion of Pt in FePt, which would yield an effective pulse width of 2.1 ms.[26] These slight differences do not appear to be critical, thus the effective pulse widths based on Fe/Pt interlayer diffusion have been used in this paper.

C. Coercivity of annealed FePt films

As previously mentioned, since the optical and thermal properties of Pt and FePt are very similar, the peak temperatures are expected to be similar for the Pt and FePt films for a given laser pulse. Consequently, the measured curves shown in Fig. 7 were used to estimate the peak temperature during the laser annealing of the FePt films. Figure 9 shows the coercivity of annealed FePt films as a function of temperature for different pulse widths. The temperatures above 700 °C were determined by extrapolation of the *R-T* calibration curve in Fig. 5. (The coercivity measurements in Fig. 9 were previously reported in Ref. 4 as a function of laser fluence.) For each pulse width, the coercivity increases with temperature reaching a maximum at about 700 °C and decreases with further increase in temperature. The peak coercivity decreases with decreasing pulse width. The peak coercivity for the 10 ms pulse was about 5.4 kOe and the peak coercivity for the 2.5 ms pulse was about 2.1 kOe. It is also worth noting that the width of the coercivity versus temperature curve decreased with decreasing pulse width. This is consistent with the shape of the TTT curve, as will be discussed later.

D. TTT curves

The average atomic order parameter, S, of the laser annealed FePt films was calculated from the ratio of the integrated (110) and (220) XRD peaks using the formula[27]

$$S^2 = \frac{(I_{110}/I_{220})_{\text{exp}}}{(I_{110}/I_{220})_{\text{calc}}}. \tag{11}$$

Figure 10 shows the order parameter as a function of peak temperature for laser pulse widths of 2.5, 5.0, 7.5, and 10 ms. The curves are qualitatively similar to those in Fig. 9 for the coercivity. The maximum order parameter occurs at about 700 °C and increases with increasing pulse width. The largest value obtained was S=0.53 using a single 10 ms laser pulse (effective time of 3.8 ms). For comparison, an order parameter near unity and a coercivity of 16 kOe could be obtained by annealing the films in a furnace for 60 s.

The longest pulse width obtainable with our pulse laser system was 10 ms. We have recently shown that the laser annealing time can be increased by using multiple pulses and that the total effective annealing time is additive.[2] This allowed us to obtain order parameters near unity using multiple pulse laser annealing. Figure 11 shows the order parameter as a function of the total effective annealing time using multiple laser pulses. The peak temperature was approximately 700 °C for each of the laser pulses, which is near the optimum annealing temperature for single laser pulses. The effective annealing time was calculated based on atomic diffusion as described earlier in this paper. The results show that the effective cumulative anneal time is approximately independent of the width of each pulse. For example, a single 10 ms laser pulse produces approximately the same order parameter as two 5 ms laser pulses or four 2.5 ms laser pulses.

The relationship between order parameter, peak temperature and effective annealing time for single laser pulses is

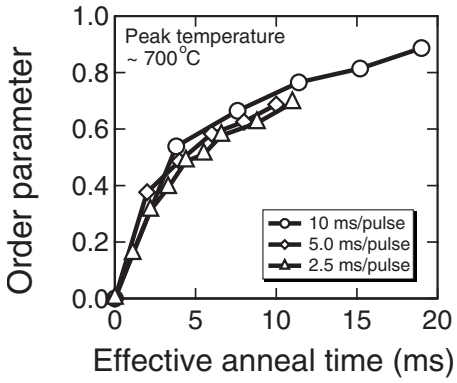

FIG. 11. Order parameter as a function of effective anneal time using multiple laser pulses.

summarized in the TTT diagram in Fig. 12. The contour curves correspond to a fixed value of order parameter. The curves were obtained by interpolation of the measured values shown in Fig. 10. The C-shapes of the curves at the minimum ordering times are in good agreement with "$k_2(T)$, N(T)" model calculations given by Berry and Barmak.[3] In particular, the location of the "nose" of the C-curve in Fig. 12 for $S=0.5$, which occurs at about $T\sim 700$ °C and $t\sim 3.5$ ms, is nearly identical to the predicted value for a 10-nm film with composition $F_{47.5}Pt_{52.5}$. It should be noted, however, that the theoretical TTT diagrams given by Berry and Barmak include volume fraction of ordered material while Fig. 12 includes the average order parameter. The model calculations of Berry and Barmak depend strongly on the film composition. For the composition $Fe_{54.4}Pt_{45.6}$ the predicted anneal time to achieve an ordered volume fraction of 0.5 is more than 100 s. Ristau *et al.*[28] measured the ordered volume fraction in 10 nm FePt films as a function of furnace anneal time at 700 °C and found that about 600 s is required for an ordered fraction of 0.5; however, their film composition was not specified. (Note that our films were nominally equiatomic based on sputtering rates and energy-dispersive x-ray spectroscopy (EDS) verification using a standard[29] and our previous atom probe analysis;[7] the experimental investigations of composition changes to the shape of the TTT diagram is the subject of future work.) The $k_2(T)$, N(T) model assumes both a temperature dependent pre-exponential factor, $k_2(T)$, for the growth velocity of the ordered domains and a temperature dependent density of ordered nuclei, N(T). The C-shape curves in Fig. 12 do not agree as well with the other models discussed by Berry and Barmak in which either N or both N and k_2 are assumed to be independent of temperature.

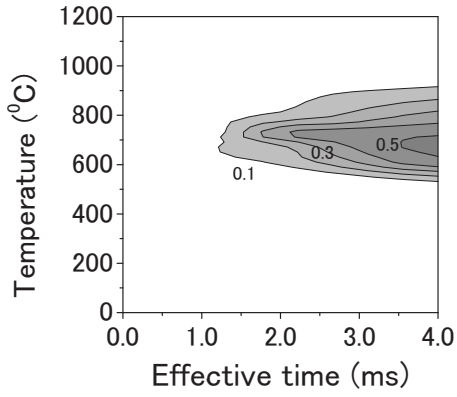

FIG. 12. TTT diagram. The numbers in contour plot indicate order parameter.

It should be emphasized that our TTT curve measurements are in the region below 4 ms and are thus not able to distinguish between models at longer anneal times. Although our multiple pulse and furnace anneals were done at longer times, the temperature was fixed at ~700 °C. Thus, these measurements are not adequate to distinguish among models for extended time scales. Reference 3 does include data at longer times and lower temperatures than the present study and those results are in better agreement with the $k_2(T)$ model or the Michaelsen–Dahms model (constant k_2). However, these measurement were done on 1 μm FeCuPt films rather than 10 nm FePt films. Since the TTT measurements depend on film composition and thickness, measurements on identical samples over a much wider range of temperature and time would be required to differentiate among the various models.

V. SUMMARY AND CONCLUSIONS

Time-temperature profiles of Pt films on glass and Si substrates produced by laser pulses have been measured. Since the film absorbencies are nearly the same, these profiles are expected to nearly mimic those of FePt. This was experimentally confirmed by the similarity of the time-temperature profiles for Pt and FePt measured with an optical pyrometer. The measured profiles are comparable to numerically calculated profiles, although the calculated peak temperatures are smaller. The temperature dependence of the resistance of the Pt film was used to estimate the temperature of the FePt films as a function of laser fluence. Both the measurements and calculations show that the cool down time of the thermal pulse is much faster for a film on glass than on Si.

Effective annealing times were calculated from the measured time-temperature transient curves based on atomic diffusion. The effective annealing times were less than one-half the laser pulse widths.

The dependence of the order parameter of pulse laser processed FePt films on peak temperature and pulse width was used to determine a section of the TTT diagram below ~4 ms. Our diagram in this regime is consistent with theoretical predictions based on a temperature dependent pre-exponential factor for ordered domain growth velocity and on a temperature dependent density of ordered nuclei. The limited range of our measurements does not allow us to compare models at longer times. The dependence of the coercivity on peak temperature and pulse width is also consistent with the TTT diagram. The measurements show partial ordering at an effective annealing time as low as 1.1 ms. To our knowledge, this study is the first to give detailed measurement of a TTT diagram for FePt that shows the lowest time limits for atomic ordering.

ACKNOWLEDGMENTS

This research was supported by the Center for Materials for Information Technology at the University of Alabama through a grant by Seagate Technologies and made use of shared facilities under NSF Materials Research Science and Engineering Center Award No. DMR–0213985. G. B. Thompson recognizes NSF Grant No. DMR-0529369 for additional support and supplies to this work. The authors gratefully acknowledge Professor Ramana Reddy for use of the Nd:YAG laser. The Tecnai TEM was acquired through the National Science Foundation Major Instrumentation Program (Grant No. DMR-0421376). Karen Henry is thanked for the preparation and image of the TEM foil shown in Fig. 1.

[1]D. Weller, A. Moser, L. Folks, M. E. Best, L. Wen, M. F. Toney, M. Schwicker, J.-U. Thiele, and M. F. Doerner, IEEE Trans. Magn. **36**, 10 (2000).
[2]B. Rellinghaus, E. Mohn, L. Schultz, T. Gemming, M. Acet, A. Kowalik, and B. F. Kock, IEEE Trans. Magn. **42**, 3048 (2006).
[3]D. C. Berry and K. Barmak, J. Appl. Phys. **101**, 014905 (2007).
[4]Y. Inaba, G. B. Thompson, J. W. Harrell, T. Klemmer, and Y. Kubota, J. Appl. Phys. **107**, 053507 (2010).
[5]Y. Inaba, S. Kang, G. B. Thompson, J. R. Izatt, I. Zana, J. W. Harrell, Y. Kubota, and T. J. Klemmer, J. Appl. Phys. **105**, 07B715 (2009).
[6]Corning 1737 AM LCD Glass Substrates Material Information (http://www.delta-technologies.com/downloads/Corning%201737.pdf)
[7]K. L. Torres and G. B. Thompson, Ultramicroscopy **109**, 606 (2009).
[8]M. A. Ordal, L. L. Long, R. J. Bell, S. E. Bell, R. R. Bell, R. W. Alexander, and C. A. Ward, Appl. Opt. **22**, 1099 (1983).
[9]K. Sato, A. Mizusawa, K. Ishida, T. Shima, and K. Takanashi, Trans. Magn. Soc. Jpn. **4**, 297 (2004).
[10]O. S. Heavens, *Optical Properties of Thin Solid Films* (Butterworth, London, 1955), pp. 76–77.
[11]J. Buschbeck, S. Fähler, M. Weisheit, K. Leistner, J. McCord, B. Rellinghaus, and L. Schultz, J. Appl. Phys. **100**, 123901 (2006).
[12]J. W. Arblaster, Platinum Metals Rev. **38**, 119 (1994).
[13]Y. Terada, K. Ohkubo, T. Mohri, and T. Suzuki, J. Alloys Compd. **285**, 233 (1999).
[14]L. A. Giannuzzi, J. L. Drown, S. R. Brown, R. B. Irwin, and F. A. Stevie, Microsc. Res. Tech. **41**, 285 (1998).
[15]Y. Inaba, K. L. Torres, S. Kang, R. Vanfleet, J. R. Izatt, J. W. Harrell, G. B. Thompson, T. Klemmer, and Y. Kubota, J. Magn. Magn. Mater. **322**, 3828 (2010).
[16]J. Trice, D. Thomas, C. Favazza, R. Sureshkumar, and R. Kalyanaraman, Phys. Rev. B **75**, 235439 (2007).
[17]T. Bååk, Appl. Opt. **21**, 1069 (1982).
[18]G. D. Mahan and D. T. F. Marple, Appl. Phys. Lett. **42**, 219 (1983).
[19]G. Hanreich and J. Nicolics, Proceedings of the IEEE Instrument and Measurement Technology Conference, Budapest, Hungary, 21–23 May 2001, pp. 1045–1050.
[20]H.-T. Chen and J.-C. Chou, Int. J. Heat Mass Transfer **49**, 3034 (2006).
[21]L. E. Greenwald, E. M. Breinan, and B. H. Kear, AIP Conf. Proc. **50**, 189 (1979).
[22]http://www.comsol.com
[23]N. Semmar and C. Boulmer-Leborgne, J. Phys. IV France **120**, 413 (2004).
[24]N. Zotov, J. Feydt, A. Savan, and A. Ludwig, J. Appl. Phys. **100**, 073517 (2006).
[25]M. Rennhofer, B. Sepiol, M. Sladecek, D. Kmiec, S. Stankov, G. Vogl, M. Kozlowski, R. Kozubski, A. Vantomme, J. Meersschaut, R. Rüffer, and A. Gupta, Phys. Rev. B **74**, 104301 (2006).
[26]J. Kučera and B. Million, Phys. Status Solidi A **31**, 275 (1975).
[27]B. E. Warren, *X-Ray Diffraction* (Addison-Wesley, Reading, MA, 1969).
[28]R. A. Ristau, K. Barmak, L. H. Lewis, K. R. Coffey, and J. K. Howard, J. Appl. Phys. **86**, 4527 (1999).
[29]C. Srivastava, J. Balasubramanian, C. H. Turner, D. E. Nikles, J. Wiest, and G. B. Thompson, J. Appl. Phys. **102**, 104310 (2007).
[30]F. Cardavelli, *Materials Handbook* (Springer-Verlag, London, 2000).
[31]A. S. Okhotin, A. S. Pushkarskii, and V. V. Gorbachev, *Thermophysical Properties of Semiconductors* (Atom, Moscow, 1972).
[32]C. J. Glassbrenner and G. A. Slack, Phys. Rev. **134**, A1058 (1964).
[33]D. E. Aspnes, in *Properties of Crystalline Silicon*, EMIS Datareviews No. 20, edited by R. Hull (INSPEC, London, 1999), p. 684.